range of the integration order to $1 \leq N \leq 15$; an optimum value for this parameter should be about 10. While compromises in numerical accuracy and efficiency between m and N are obvious, no practical rule yielding optimum values of these parameters (for a particular orbit case) has yet been determined. Experience with various types of orbital trajectories may furnish such a rule.

The integration mode used should normally be *predict–pseudo correct* (P–PC). The important difference in the modes is that DPTRAJ integrates one orbit per multirevolution step in the P and P–PC modes, but must integrate twice per step in the P–C mode. The expense of a DPTRAJ integration (well over 90% of the total computer time required for a multirevolution step), and the relatively small gain in accuracy by the use of P–C over P–PC, should limit the use of the P–C mode.

Printed output appears once every h orbits (starting with the first), and consists of the five osculating Kepler elements, a, e, i, Ω, ω, the current trajectory time in Ephemeris Time, and the orbit number k. The sixth element, T, is zero, since periapsis is the reference point. The reference coordinate plane for the elements is the mean earth equator of 1950.0, the coordinate system used by DPTRAJ in the single-orbit integration. Other standard two-body orbital parameters, such as c_1 and c_3, will be available. The capability to plot individual orbital elements versus the revolution number k will also be available as a user option.

Restrictions in the use of LEAP are:

(1) The increments in the orbital elements over one revolution, $\Delta\mathbf{a}$, must be sufficiently "smooth" functions of the revolution number k so that the functions $f(\mathbf{a}, k) = \Delta\mathbf{a}$ can be adequately represented by polynomials of fixed degree over a substantial range of values of k. This corresponds physically to the assumption that the perturbing forces vary smoothly and slowly from orbit to orbit. Thus, the technique may not adequately account for perturbing forces which are not near-periodic with respect to the orbital period of the probe. Such a perturbing force would be that due to tesseral harmonic gravitational terms associated with a nonspherical central body with a rotational period not small compared to the orbital period of the probe.

(2) The initial conditions input to the program must correspond to an elliptical orbit.

(3) The starting procedure for the multirevolution integration is a compromise between machine time efficiency and numerical precision. The resulting number of single orbits, J, computed by DPTRAJ (in P–PC mode) during this starting process is equal to $Ns + 1$, where s is the smallest integer such that $2^{s-1} \geq m$. Thus for the case $N = 10$, $m = 100$, we have $J = 81$.

(4) The interpolation procedure allows the computation of the state vector at grid points intermediate to the large grids. Interpolation is *not* valid for computing the state at time points between the fine grids (i.e., at any point on the orbit other than periapsis) since the functions $\mathbf{f}_{nm} = \Delta\mathbf{a}_{nm}$ are not defined between fine grid points.

(5) The computer time required for a given case depends heavily on the choice of m and N, and of course, on the total number of revolutions integrated.

B. Communications System Research

1. Ranging With Sequential Components, *R. M. Goldstein*

a. Introduction. The JPL ranging system is being redesigned with the goal of extending its capability to weaker thresholds without lowering its present high level of accuracy. Simplicity of design is also considered an important goal.

Sequential components allow the full ranging power to be available for each step of the search. Power does not have to be shared among the components. A further advantage is freedom from combinatorial restrictions; i.e., the component lengths need not be relatively prime. Square waves (sequences of length 2) have been chosen for all of the components.

b. Method. This system has been designed so that the RF carrier loop provides the entire tracking function. The receiver coder is geared to the received RF so that the coder necessarily runs at the same rate as the received code. The time of flight measurement is then made open loop.

Figure 30 is a functional block diagram of the system. Here f_c, a submultiple of the transmitted frequency, is the clock for the transmitter coder. The RF doppler is multiplied by a fixed ratio to provide the proper frequency for the code doppler.

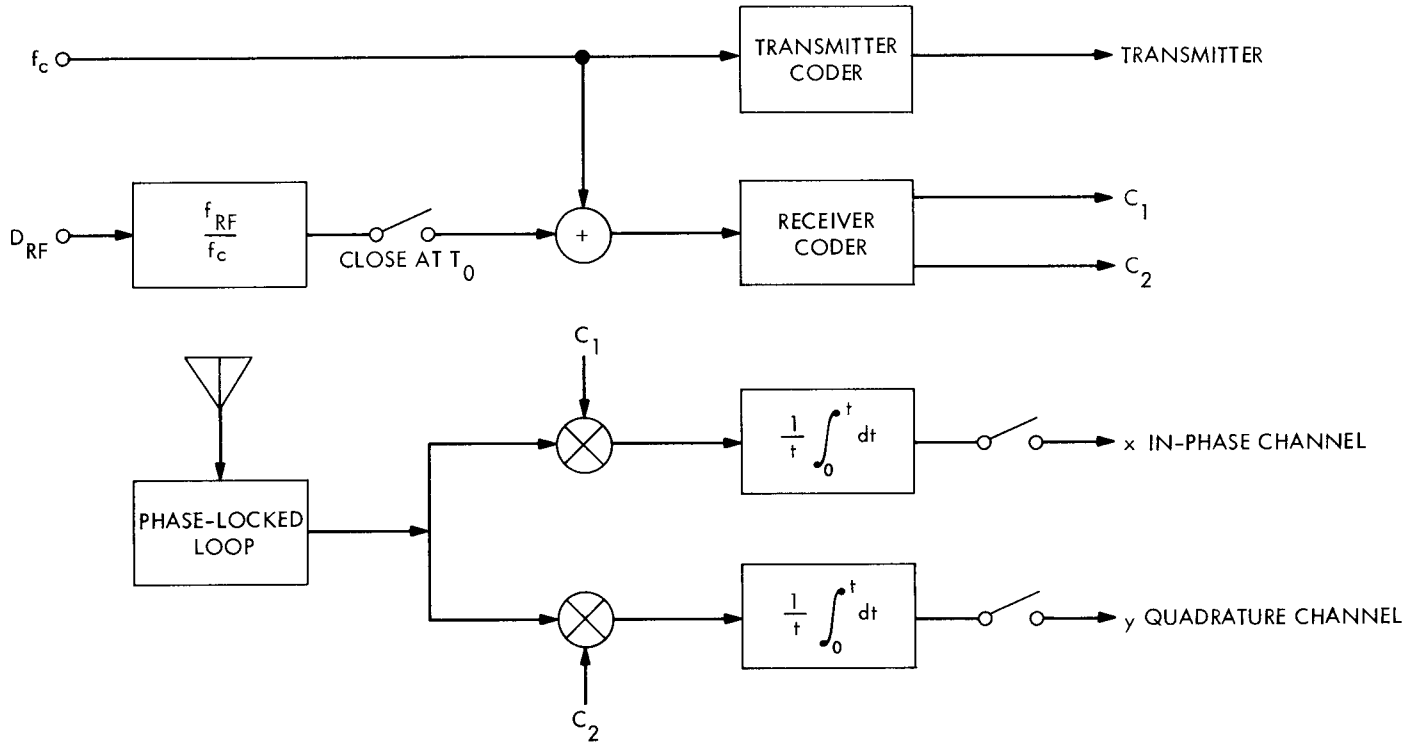

Fig. 30. Functional block diagram of the ranging system

The system operates as follows: With the doppler switch open, the two coders are synchronized. At time t_0 the switch is closed. Thereafter, the timing between the receiver coder and the received code remains fixed. This time difference (measured at leisure) represents the time-of-flight (TOF)[10] of the signal at t_0.

The two receiver channels serve to measure the phase between the received square wave and the receiver coder square wave. This technique parallels closely the optimum phase estimator for a sine wave signal. After t seconds, the integrator outputs x and y are sampled. Figure 31 is a graph of the dependence of x and y on the time difference τ. It is easily shown that

$$\tau = \frac{y}{x+y}\frac{T}{2} \tag{1}$$

where T is the bit period, and (x, y) has been assumed in the first quadrant. A similar formula holds for each quadrant.

[10]TOF at t_0 is ambiguous unless one specifies whether it pertains to the wave arriving at t_0 or to the one leaving. Conventionally, we use the former, or "backward looking," TOF.

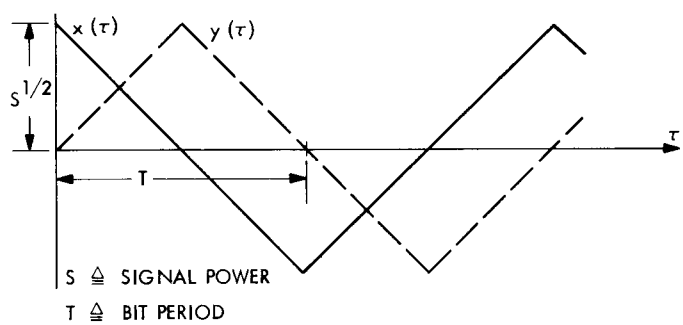

Fig. 31. Integrator outputs plotted as a function of the transmitter coder–receiver coder time difference

There is, of course, an ambiguity in the measurement. Since the first (and shortest) component length is 2 μs, an unknown multiple of 2 μs must be added to the TOF. To resolve this, the receiver coder is switched to the next slower square wave (the transmitter coder having been so switched one TOF previously). This procedure is iterated; each time the integrator outputs (x_i, y_i) are used to remove part of the previous ambiguity. The process terminates when the *a priori* knowledge removes the balance of the ambiguity.

c. Accuracy. In the discussion so far, noise has not been considered. The integrator outputs are only estimates of

the noise-free case, and

$$\hat{x} = x + n$$

$$\hat{y} = y + m$$

where n and m are independent zero mean gaussian variates of variance

$$\sigma_n^2 = \sigma_m^2 = N_0/2t \tag{2}$$

where N_0 is the one-sided noise density, and t is the integration time.

We use the simple approximation

$$\sigma^2 = \left(\frac{\partial\tau}{\partial\hat{x}}\right)^2 \sigma_{\hat{x}}^2 + \left(\frac{\partial\tau}{\partial\hat{y}}\right)^2 \sigma_{\hat{y}}^2$$

evaluated at $\hat{x} = x$, $\hat{y} = y$ and Eq. (1) to find that the variance of the estimate

$$\hat{\tau} = \frac{\hat{y}}{\hat{\tau} + \hat{y}} \frac{T}{2}$$

of τ is approximately

$$\sigma^2 = T^2 N_0/8st \tag{3}$$

where s is the power in the ranging signal.

d. Component periods. We now consider the following problem: Should the integration time t be long so that fewer square waves with widely spaced periods need be examined; or should many square waves be examined so that t may be short?

The uncertainty of the time measurement, σ_i, at each step need only be small enough to remove the ambiguity of all of the preceding steps (which equals the previous bit time T_{i-1}).

$$k\sigma_i = T_{i-1} \tag{4}$$

The factor k provides a margin, or confidence level. Using Eqs. (3) and (4), we have

$$T_i \left(\frac{a}{t_i}\right)^{1/2} = T_{i-1}$$

and

$$T_{i+1} \left(\frac{a}{t_{i+1}}\right)^{1/2} \left(\frac{a}{t_i}\right)^{1/2} = T_{i-1}$$

$$\vdots$$

$$T_n \left(\frac{a^n}{t_1 t_2 \cdots t_n}\right)^{1/2} = T_0 \tag{5}$$

where $a = k^2 N_0/8s$.

Thus after n steps the uncertainty has been reduced by the factor

$$(t_1 t_2 \cdots t_n/a^n)^{1/2} \tag{6}$$

The total time required for these n steps is

$$t_1 + t_2 + \cdots + t_n \tag{7}$$

Using the Lagrange multiplier technique to maximize Eq. (6) while holding Eq. (7) constant, for fixed n one easily finds that all of the t_i must be equal. Then the advantage becomes

$$(t^n/a^n)^{1/2} \tag{8}$$

and the penalty becomes

$$nt \tag{9}$$

Again, the Lagrangian technique of maximizing Eq. (8) while holding Eq. (9) constant (assuming n a continuous variable), shows that

$$t/a = e$$

Since the ratio of successive periods, from Eq. (5), is $(t/a)^{1/2}$ we see that the ratio

$$T_n/T_{n-1} = e^{1/2} = 1.65 \cdots \tag{10}$$

We choose the convenient nearby integer 2. Hence each of the sequential components of this system has twice the period of the previous one.

e. Probability of error. As we have seen, the first highest speed component serves to measure the time delay with the most precision. Each successive component then removes half of the ambiguities left by all of the previous components. We next consider the probability of making an error in any of the components 2 through n. Any such error would invalidate the entire TOF measurement.

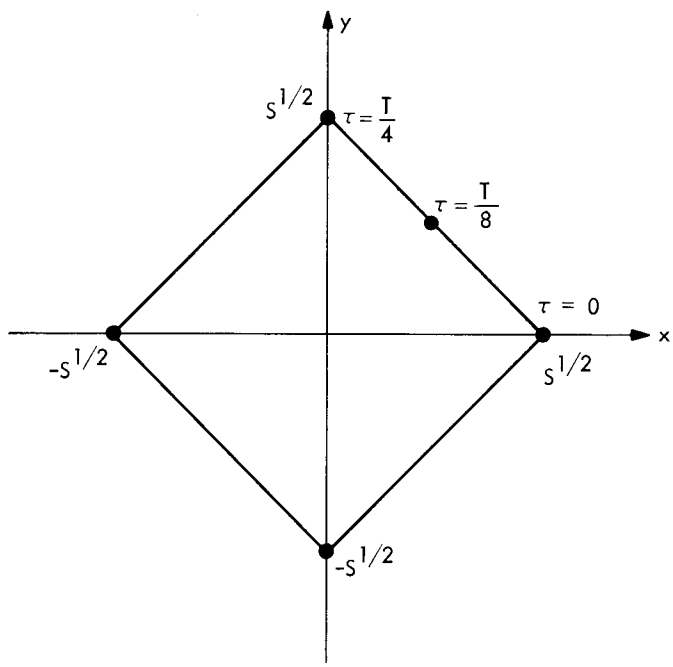

Fig. 32. Integrator outputs plotted against each other, with time difference as a parameter

Figure 32 shows the integrator outputs x and y plotted against each other, with τ as a parameter, in the noise-free case. If the previous measurements happen to give $\tau = 0 +$ (multiple of $T/2$), the current measurement need only distinguish between the two points $(s^{1/2}, 0)$ and $(-s^{1/2}, 0)$. The answer will be correct if, and only if, $x > 0$. This will happen with probability

$$p\,(\text{correct}) = \frac{1}{\pi^{1/2}} \int_{-\infty}^{(st/N_0)^{1/2}} e^{-z^2}\,dz \qquad (11)$$

The same result applies if the previous measurements had shown that $\tau = T/4$, $T/2$ or $3T/4 +$ (multiple of $T/2$). However, if $\tau = T/8 +$ (multiple of $T/2$), the current measurement must distinguish between the closer points $(s^{1/2}/2, s^{1/2}/2)$ and $(-s^{1/2}/2, -s^{1/2}/2)$.

One can see from Fig. 32 that the answer will be correct whenever $y > -x$. The probability of this event is

$$p\,(\text{correct}) = \frac{1}{\pi^{1/2}} \int_{-\infty}^{(st/2N_0)^{1/2}} e^{-z^2}\,dz \qquad (12)$$

A comparison with Eq. (11) shows a 3-dB loss in this case. In order to avoid this loss, the receiver coder is shifted by the amount measured with the first component. Thereafter τ will always equal $0 +$ (multiple of $T/2$). The

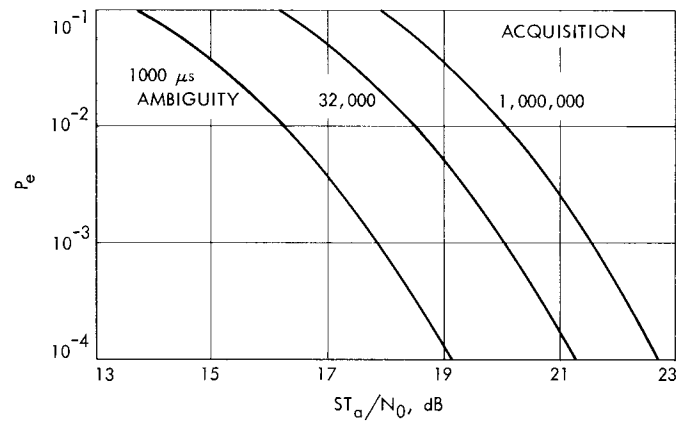

Fig. 33. Probability of an error in resolving the code ambiguities

probability of at least one error is then

$$p_e = 1 - p\,(\text{correct})^{n-1}$$

where n is the total number of components.

Figure 33 is a graph of the probability of error as a function of the total acquisition energy-to-noise-density ratio. The final component period (hence the final ambiguity time) is taken as a parameter.

f. Conclusions. We have described a ranging system which uses sequential square wave components. The shortest has a period of 2 μs and each successive component has double the period of the preceding one. The entire tracking function is performed by the RF carrier loop, leaving the time delay measurements to be done open loop. Formulas have been given for the precision of the delay measurement as well as the probability of erroneously resolving any of the ambiguities.

As an example, suppose it were desired to range *Mariner V* at encounter with this system. Suppose that 25 min were available to range to ±15 m with 1 sec of ambiguity and 0.0001 probability of error. Then with $S/N_0 = 0.206$, the first component would require 1 min, and components 2 through 19 would require a total of 15 min. The round trip time was 9 min. The actual S/N_0 was 101, a margin of 27 dB.

2. Ephemeris-Controlled Oscillator Analysis, *K. D. Schreder*

a. Introduction. An ephemeris-controlled oscillator (ECO) is a sampled-data phase control system in which the output phase is controlled by the input phase. The